

Maderas-Cienc Tecnol 22(3):2020
Ahead of Print: Accepted Authors Version

DOI:10.4067/S0718-221X2020005XXXXXX

ESTIMATION OF MOISTURE IN WOOD CHIPS BY NEAR INFRARED SPECTROSCOPY

Evelize A. Amaral^{*1}, Luana M. Santos¹, Paulo R. G. Hein¹, Emylle V. S. Costa¹,
Paulo F. Trugilho¹

¹Department of Forestry Sciences – Wood Science and Technology, Lavras
University, Street Address, Lavras, Minas Gerais, 372000-000, Brazil

*Corresponding author: paulo.hein@ufla.br

Received: August 12, 2019

Accepted: March 31, 2020

Posted online: Abril 01, 2020

ABSTRACT

In order to assess the moisture content of wood chips on an industrial scale, readily applicable techniques are required. Thus, near infrared (NIR) spectroscopy was used to estimate moisture in wood chips by means of partial least squares regressions. NIR spectra were obtained in spectrometer with an integrating sphere and optical fiber probe, on the longitudinal and transverse surface of *Eucalyptus* wood chips. The specimens had their masses and NIR spectra measured in 10 steps during drying from saturated to anhydrous condition. Principal Component Analysis was performed to explore the effect of moisture of wood chip on NIR signatures. The values of moisture content of chips were associated with the respective NIR spectra by Partial Least Squares Regression (PLS-R) and Partial Least Squares Discriminant Analysis (PLS-DA) to estimate the moisture content of wood chips and its moisture classes, respectively. Model developed from spectra recorded on the longitudinal face by the integrating sphere method presented statistics slightly better ($R^2_{cv} = 0,96$; $RMSE_{cv} = 7,15 \%$) than model based on optical fiber probe ($R^2_{cv} = 0,90$; $RMSE_{cv} = 11,86 \%$). This study suggests that for calibration of robust predictive model for estimating moisture content in chips the spectra should be recorded on the longitudinal surface of wood using the integrating sphere acquisition method.

Keywords: Cellulose, integrating sphere, optical fiber, paper, physical properties,

35 **RESUMEN**

36 Para evaluar el contenido de humedad de las astillas de madera a escala industrial, se
37 requieren técnicas fácilmente aplicables. Por lo tanto, se utilizó la espectroscopía de
38 infrarrojo cercano (NIR) para estimar la humedad en astillas de madera mediante
39 regresiones parciales de mínimos cuadrados. Los espectros NIR se obtuvieron en un
40 espectrómetro con una esfera de integración y una sonda de fibra óptica, en la superficie
41 longitudinal y transversal de las astillas de madera de *Eucalyptus*. Las muestras tenían
42 sus masas y espectros NIR medidos en 10 pasos durante el secado de condición saturada
43 a anhidra. Los valores del contenido de humedad de las astillas se asociaron con los
44 espectros NIR respectivos mediante Regresión Parcial de Mínimos Cuadrados (PLS-R)
45 y Análisis Discriminante de Mínimos Cuadrados Parciales (PLS-DA) para estimar el
46 contenido de humedad de las astillas de madera y sus clases de humedad,
47 respectivamente. El modelo desarrollado a partir de espectros registrados en la cara
48 longitudinal por el método de la esfera integradora presentó estadísticas ligeramente
49 mejores ($R^2_{cv} = 0,96$; $RMSE_{cv} = 7,15 \%$) que el modelo basado en una sonda de fibra
50 óptica ($R^2_{cv} = 0,90$; $RMSE_{cv} = 11,86 \%$). Este estudio sugiere que para la calibración
51 de un modelo predictivo robusto para estimar el contenido de humedad en las astillas,
52 los espectros deben registrarse en la superficie longitudinal de la madera utilizando el
53 método de adquisición de esfera integradora.

54 **Palabras clave:** Celulosa, esfera integradora, fibra óptica, Papel, propiedades físicas.

55

56 **INTRODUCTION**

57 Although moisture is not an intrinsic characteristic of wood, it is among its most
58 important properties, because its variation affects the behavior of the material during
59 the industrial processing and application phases (Tsuchikawa and Schwanninger 2013).
60 In industries that use wood chips as raw material, the knowledge of moisture is an
61 important parameter of quality, since in addition to guaranteeing the quality of the final
62 product, it reduces losses and costs with reagents (Fardim 2005).

63 In the cellulose and paper industry, although it is not a limiting factor in the
64 Kraft pulping process, the knowledge of the moisture of the chips is essential to make
65 adjustment calculations in the process. Moisture values are important to determine the
66 dry mass of the chips correctly and to calculate the quantity of the cooking reagents,
67 and their correct ratio of wood liquor (Gomide and Fantuzzi Netto 2000).

68 Biermann (1996) also emphasizes the importance of knowledge and the control
69 of moisture in the costs of transportation and commercialization of raw material. The
70 influence is observed in situations where the purchase of chips is carried out by weight,
71 in this way, the greater the moisture of the material, the lower the amount of raw
72 material purchased.

73 To perform the monitoring of water contents in the wood, it is necessary to adopt
74 techniques that are fast, efficient and inexpensive, in order to obtain improvements in
75 the quality of the final product (Muñiz *et al.* 2012). The methods currently available are
76 time-consuming, making it difficult to control the drying process for a large quantity of
77 raw material.

78 The principle of operation of the NIR technique consists of exposing a specimen
79 to the near infrared region spectrum, the generated spectra contain data of the chemical
80 constituents of the material that, when related to the results of conventional analyzes,
81 generate statistical models that explain most this information in the spectra (Price *et al.*
82 2001; Pavia *et al.* 2010; Pasquini 2018). Thus, it is possible to estimate several
83 properties contained in biological materials, such as wood (Dahlbacka and Lillhonga
84 2010; Arriel *et al.* 2019; Tyson *et al.* 2012; Tsuchikawa and Schwanninger 2013;
85 Tsuchikawa and Kobori 2015).

86 Some studies were carried out using near infrared spectroscopy (NIR) to
87 estimate wood moisture. Thygesen and Lundqvist (2000) have investigated the thermal
88 effects on NIR spectra for estimating moisture content in *Picea abies* wood under
89 temperature conditions varying between -20 °C and +25 °C. Eom *et al.* (2013) applied
90 the NIRS technique to measure the surface moisture of poplar wood of *Populus* specie
91 during desorption conditions. Fujimoto *et al.* (2012) evaluated the NIR spectra obtained
92 from specimen *Larix kaempferi* containing different amounts of water were used to
93 verify the effect of moisture conditions on the accuracy of the estimated density of the
94 wood. Watanabe *et al.* (2011) applied the NIR technique for classification based on
95 moisture from green spruce wood. The authors have shown that NIR spectroscopy has
96 the potential to estimate the mean green wood moisture, although it only provides
97 values of surface moisture content. Karttunen *et al.* (2008) reported a survey of the
98 moisture distribution in two sets of wild pine trunks using NIR spectroscopy. Moisture
99 variation among trees was detected with high precision. Tham *et al.* (2018) carried out
100 a study applying the capacitive method and the NIR spectroscopy together to
101 simultaneously predict the density and moisture of wood specimens. The results suggest
102 the possibility of a new device combining the capacitive method and the NIR
103 spectroscopy to predict density and moisture with greater accuracy.

104 These studies have pointed to NIR spectroscopy as a promising alternative in
105 the estimation of wood moisture. However, the influence of the anisotropy of the
106 material and the path of spectral acquisition in the characterization of the wood chips
107 via spectroscopy in the NIR is not yet fully understood. Therefore, it is necessary to
108 know these parameters in order to develop predictive models based on moisture in wood
109 chips in order to maintain the quality of the raw material and contribute to the industries

110 that use wood chips in their production, reducing costs with reagent and reducing water
111 consumption.

112

113 **EXPERIMENTAL SECTION**

114 **Wood chips and water desorption monitoring**

115 Forty (40) wood chips from *Eucalyptus urophylla* and *Eucalyptus grandis*
116 hybrids of different ages and sizes were used. The chips present, in average, the
117 following dimensions: 35 mm wide, 25 mm long (longitudinal direction) and 3 mm - 4
118 mm thick. The selection was performed according to the wood chips that presented
119 better conditions on their surfaces for the acquisition of the spectra.

120 The specimens were identified and submitted to saturation in a vessel with water,
121 which was changed periodically for 30 days until complete saturation. The moisture of
122 the specimens was performed in 10 steps during drying of according to the gravimetric
123 method described in NBR 14929 (ABNT 2017).

124 In the first phase, the saturated test specimens were submitted to natural drying
125 until reaching equilibrium moisture (~12 %). Mass measurements and spectral
126 acquisition were performed when the control specimens lost about 10 % of the mass as
127 a function of the pre-determined anhydrous mass. After reaching equilibrium moisture,
128 the test specimens were subjected to drying in an oven at $50\text{ }^{\circ}\text{C} \pm 2\text{ }^{\circ}\text{C}$ until the control
129 specimen lost approximately 10 % of the mass in relation to anhydrous mass, according
130 to the procedure described in Santos (2017).

131 **Recording NIR spectra**

132 The spectral acquisition was performed in a diffuse reflection mode using a
133 Fourier transform spectrometer. The spectrometer has two acquisition paths: integrating

134 sphere and optical fiber probe. The spectra were captured in the near infrared region,
135 opening the range of 12500 cm^{-1} to 4000 cm^{-1} , with spectral resolution of 3845 cm^{-1} and
136 32 scans for reading according to Costa *et al.* (2018).

137 The spectra were captured during the 10 drying steps, at every 10 % mass loss
138 of water using the fiber optical probe on longitudinal and transverse surface of the
139 material. For acquisitions based on integrating sphere, NIR spectra were taken only on
140 longitudinal surface of wood. It was not possible to record NIR spectra on the transverse
141 surface of chips due to the difficulty of positioning the specimen on scanner window.

142 Individual chip specimens were investigated instead to analyze chip batches in
143 order to reduce the possible noise level in the signal. NIR were recorded from an optical
144 fiber probe or integrating sphere directly on the single chip surface. When using a
145 portion of chips, there is a lot of empty space between the chips and between the sensor
146 and the wood surface, generating noise in the signal.

147

148 **Multivariate statistics**

149 Principal Component Analysis (PCA), Partial Least Squares Regression (PLS-
150 R) and the Partial Least Squares Discriminant Analysis (PLS-DA) were developed in
151 the free software Chemoface version 1.61 (Nunes *et al.* 2012).

152 PCA was used to evaluate the effect of the presence of water in the wood chips
153 are in their spectral signature. PLS-R was developed to associate spectra with the chip
154 moisture values determined by gravimetric method and generate a regression capable
155 of estimating continuous values of moisture based on the NIR spectra recorded on the
156 chips. PLS-DA model was held in order to classify their moisture in three (3) categories
157 of moisture (up to 40 %, between 40 % and 80 %, and above 80 % moisture content)
158 based on NIR spectrum signature.

159 Analyzes were performed separately for the spectra obtained in the longitudinal
160 and transverse surfaces of the specimens and by two methods of spectral acquisition:
161 integrating sphere and fiber optic probe.

162 After adjusting several preliminary models, six latent variables (LV) calculated
163 from 1300 spectroscopic variables were used for all models. Thus, the presented models
164 were developed with these six (6) latent variables for calibrations and validations. To
165 select the best predictive models the following criteria were adopted: coefficient of
166 determination of the cross-validation model (R^2CV), root mean standard error of cross-
167 validation (RMSECV) and the ratio of performance to deviation (RPD), as described in
168 Rosado et al. (2019). The independent and cross-validation methods were used to test
169 the robustness of the estimates. Leave one out method was used for full cross
170 validations while for independent validation was done using 2/3 of samples chosen at
171 random for calibrations and 1/3 of remaining specimens for test set validation.

172 The calibrations were performed from the original (untreated) spectra and the
173 mathematically treated spectra by the first derivative method using Savitzky–Golay
174 algorithm with 13-point filter and a second-order polynomial, as described in Costa *et*
175 *al.* (2018). Moreover, the wavenumbers from 12000 cm^{-1} to 9000 cm^{-1} were not
176 considered. That process had the purpose eliminate noise and improve the quality of
177 the calibration signal.

178

179

180

181

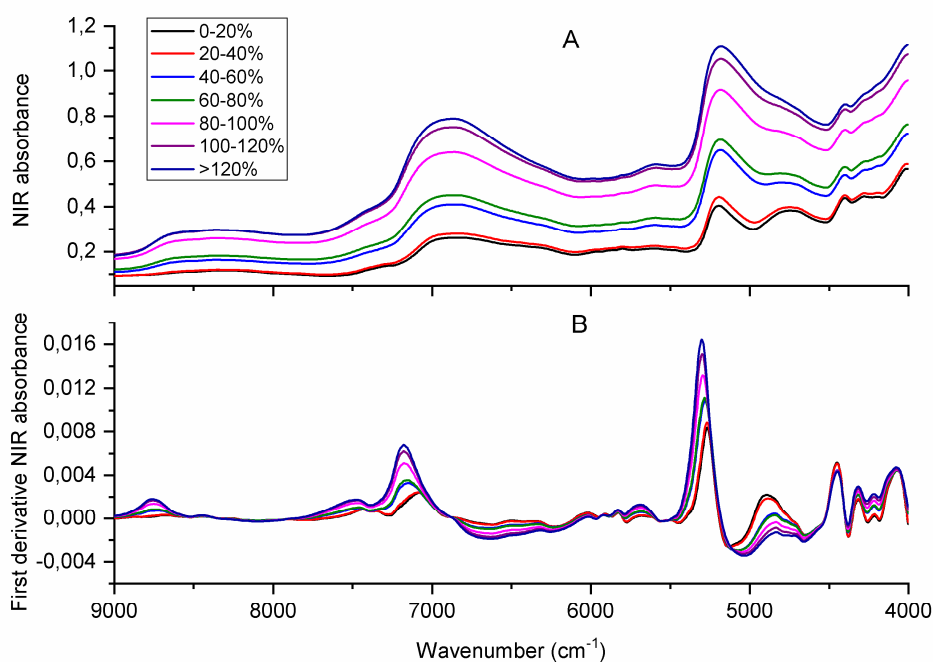
182

183

184 RESULTS AND DISCUSSION

185 Effect of moisture on spectral signature

186 Figure 1 shows diffuse reflectance spectra of wood chips obtained on the
187 longitudinal face using the integrator sphere acquisition path in different moisture
188 classes, with the original data and after the mathematical treatment of the first derivative.
189 The first derivative is able to identify differences in moisture classes in wood chips.



190 **Figure 1:** Diffuse reflection spectra obtained with the original (untreated) data (A)
191 and with the treatment of the first derivative (B).

192 Absorption peaks can be observed at wavelengths of approximately 7000 cm^{-1}
193 and 5100 cm^{-1} or (1428 and 1960) nm. These values are consistent with the results
194 obtained by Watanabe *et al.* (2011) that found greater absorption at the wavelength of
195 1430 nm and 1910 nm. The variation in these absorption peaks can be associated with
196 variation in moisture content, since they indicate vibrations characteristic of hydroxyl
197 groups – OH present in water. These peaks increase with increasing chip moisture.

198 According to Karttunen *et al.* (2008) water absorption bands occurs mainly
199 due to changes in the free water content in capillaries, because different water levels

200 can modify the NIR spectrum when incident light is spread on the surface of the
201 specimen.

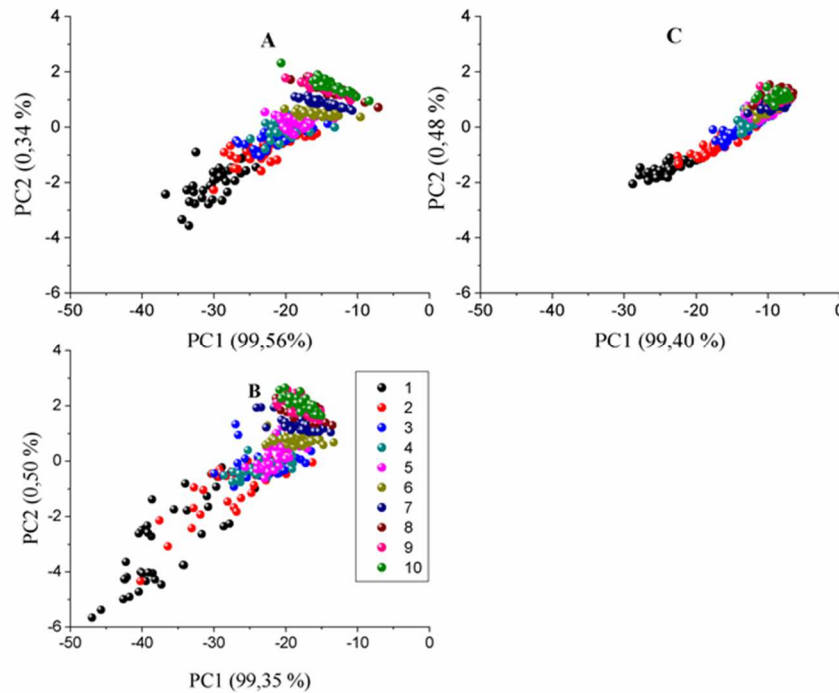
202 According to Adedipe and Dawson-Andoh (2008) a higher or lower spectral
203 range has no significant influence on moisture prediction, from which the range
204 encompasses water absorption bands. The same authors, when limiting the spectral
205 range from 1400 nm to 1940 nm, predicted the water content in the wood with similar
206 precision when they used a range 800 nm to 2500 nm.

207 **Principal component analysis**

208 The principal component analyzes (PCA) were carried out with original spectra
209 obtained through the two acquisition pathways (integrator sphere and optical fiber) in
210 the longitudinal and transverse faces of the wood chips, to carry out a preliminary
211 evaluation of the behavior of the spectra and possible separation of the specimens
212 according to the 10 moisture steps ranging from 1 (saturated condition) to 10
213 (anhydrous condition) Figure 2.

214 The two main components together account for approximately 100 % of the
215 variability of the analyzed data on the longitudinal side of both acquisition pathways,
216 99,35 % are explained by the main component 1 (PC1) and 0,50 % is explained by the
217 main component 2 (PC2) in the fiber optic acquisition pathway. with regards to the NIR
218 spectra taken by the integrating sphere, 99,40 % of variance was explained by PC1 and
219 0,48 % by PC2.

220 The integrating sphere in the longitudinal face was able to differentiate better
221 the specimen with different moisture, generating less overlaps. The wettest specimens
222 were more dispersed in relation to the drier specimens. This was due to the existence
223 of similar moisture in these measurement steps.



224 **Figure 2:** Graphic of scores obtained by PCA applied to the spectral information
225 measured in the wood chips from the optical fiber probe acquisition path on the
226 longitudinal face (A) transverse surface (B) and from the acquisition path acquisition
227 integrating sphere longitudinal surface (C).

228 Global model for estimating chip moisture

229 Table 1 presents the statistics associated to calibrations and cross validations for
230 estimating the wood chip moisture from the original spectra and treated with the first
231 derivative.

232 The spectra-based models in the NIR were efficient for estimating moisture in wood
233 chips with errors between 7,15 % and 11,86 %. The longitudinal face is the most
234 suitable for spectral acquisition, since the estimation error is smaller when compared to
235 the transverse face, besides the operational ease of measurement. However, the
236 transverse face can also be used in the estimation of moisture, since they presented
237 acceptable RPD of 3,16. According to Sobering and Williams (1993) with calibrations
238 with RPD values between 2 and 3 indicate that the predictions are approximate and
239 values between 3 and 5 indicate that the calibrations are satisfactory for the predictions.

240

241 **Table 1:** Calibrations and cross-validations for moisture estimation in wood chips.

Model	Via of acquisition	Surface	Treat.	R ² cal	RMSEc %	R ² cv	RMSEcv %	RPD
1	Sphere	Long	-	0,95	7,54	0,95	7,78	4,82
2			1d	0,96	6,79	0,96	7,15	5,24
3	Fiber	Long	-	0,94	9,08	0,93	9,38	4,00
4			1d	0,94	9,17	0,93	9,61	3,90
5		Trans	-	0,90	11,30	0,89	11,60	3,23
6			1d	0,90	11,29	0,90	11,86	3,16

Treat - mathematical treatment; 1d - first derivative; R²c - coefficient of determination of the calibration; RMSEc - Root mean square error of calibration; R²cv - coefficient of determination of the cross-validation; RMSEcv - Root mean square error of cross-validation; RPD - ratio performance to deviation; Long - longitudinal surface and Trans - transverse surface.

242 Regarding the spectral acquisition method, the calibrations developed from the two
 243 types of spectra in the NIR (integrator sphere and fiber optic) have the potential to
 244 satisfactorily estimate the moisture of the wood. However, the models generated from
 245 the spectra obtained by integrator sphere (models 1 and 2) presented more satisfactory
 246 statistical results (R²CV higher than 0,95 and RMSECV lower than 7,77 %).

247 The models generated from the first derivative of the spectra (models 2, 4 and
 248 6) provided better estimates. Martens and Naes (1991) argue that mathematical
 249 treatments aim to improve signal quality and reduce noise. However, it is observed that
 250 there was no significant improvement in the spectra of the wood chips via optical fiber
 251 treated with the first derivative.

252 In general, the model generated by the spectra of the integrating sphere
 253 presented better statistics than those generated by optical fiber probe. According to
 254 Costa (2018) this difference between the models can be explained from the comparison
 255 between the areas of the acquisition path ways. The integrating sphere acquisition
 256 pathway has a circular area with a diameter of 10 mm, while the fiber optic acquisition
 257 pathway has a circular area of approximately 1 mm in diameter. The higher value area

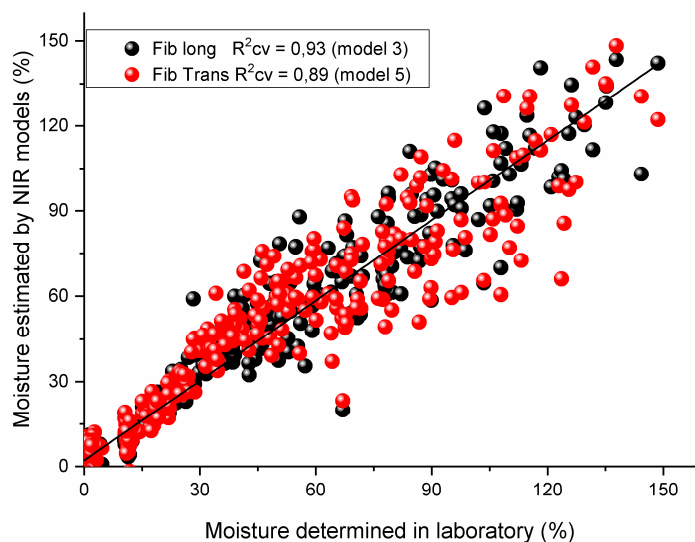
258 allows better representation of the surface of the wood chips. In this way, this path
259 becomes better suited to acquire spectra in order to estimate moisture in wood chips.

260 The wood surface that presented the best results, in both acquisition pathways,
261 was longitudinal. This result differed from some authors, such as Defo *et al.* (2007)
262 who used near-infrared spectroscopy to determine the moisture of *Quercus* spp. (red
263 oak) by means of spectra collected on the radial, tangential and transverse face. When
264 comparing the prediction of the models generated in the different faces, the authors
265 realized that the transversal face was the one that obtained the best performance. This
266 difference in results may have occurred due to the raw material of the authors being
267 lumber, whereas the one used in the study is wood in the form of wood chips.

268 Figure 3 shows the relationship between moisture estimated by the NIR and
269 determined in the laboratory from the optical fiber probe, on both surfaces (longitudinal
270 and transverse) of the wood chips. The prediction accuracy is higher in specimens with
271 moisture content lower than 30 % (Figure 3). Yang *et al.* (2014) have reported fiber
272 saturation point of 29 % for *Eucalyptus urophylla* wood. Thus, we supposed that the
273 spectral change in lower moisture content is mainly due to the decrement of absorbed
274 water whereas in higher moisture content spectral change is resulted in the change of
275 free water.

276 The cross-validation values obtained by the acquisition of spectra in the
277 integrating sphere presented values similar to the measured values of moisture in the
278 laboratory (Figure 3). However, it was observed that the cross-validation performed by
279 the longitudinal face presented a better distribution of the data ($R^2 = 0,93$), when
280 compared with the transversal face that presented the lowest performance ($R^2 = 0,89$).
281 This result may have occurred due to the fact that the longitudinal face presents a rough

282 surface in relation to the transverse face, since the roughness may have facilitated the
283 penetration of light in the chips.



284 **Figure 3:** Moisture of the wood chips determined in the laboratory and
285 estimated in the NIR from the optical fiber according to models 3 and 5 of Table 1.

286
287 Zhang *et al.* (2015) studied the correlation between NIR spectroscopy and the
288 surface roughness of the wood. The authors used optical fiber to obtain the spectra. The
289 results showed that the roughness of the surface of the wood can influence in the
290 statistics to estimate the properties of the wood from NIR spectroscopy. Greater surface
291 roughness may be associated with more pronounced diffuse reflection.

292 The longitudinal face through the integrating sphere presented the best model in
293 the PLS-R analysis, so it was divided into three ranges of moisture (0 % to 40 %, 40 %
294 to 80 %, and > 80 % moisture) for to generate models capable of predicting wood
295 moisture by classification using PLS-DA.

296 Model 2 of Table 1 was applied in the NIR spectra of specimens to generate estimates.
297 Specimens were separated into 3 classes (0 % to 40 %, 40 % to 80 %, and > 80 %)
298 based on the predicted moisture content by model 2 and a confusion matrix was
299 presented in Table 2 to evaluate the correct classification ratio.

300 **Table 2:** Confusion matrix of predictions of chip moisture based on NIR spectra
 301 through model 2 (Table 1).

Nominal Moisture classes (%)	Moisture estimated by model 2 (%)			Correct classification		Total specimens
	0 - 40	40 - 80	> 80	No.	%	No.
0 - 40	203	6	6	203	94,4	215
40 - 80	12	71	12	71	84,5	84
> 80		7	89	89	88,1	101
Total	215	83	107	363	90,7	400

302

303 The confusion matrix (Table 2) shows that 363 from 400 (90,7 %) of specimens were
 304 correctly classified based on PLS-R model 2 (Table 1). 203 from 215 chips had their
 305 estimated moisture value correctly classified within the class of drier samples (0 to
 306 40) %. In the class of samples with intermediate humidity (between 40 and 80), 84 %
 307 of the samples were correctly classified by model 2 of Table 1. Finally, in the class of
 308 the most humid samples, 89 of 101 samples were correctly classified and only 7 samples
 309 (6,9 %) had moisture estimates that classified them as intermediate samples.

310 This approach is very useful for pulp and paper companies that need to have a tool that
 311 allows them to separate chips into batches of different moisture quickly and reliably.

312 **Model for estimating the moisture of the wood chips per class**

313 Table 3 shows the regression models obtained by calibration and cross-
 314 validation from the spectra with and without first derivative treatment.

315 Table 3 shows that the first moisture class of (0 to 40) % was the one that
 316 presented the best estimates of wood moisture, especially when submitted to the
 317 treatment of the first one derivative, resulting in R²CV of 0,96 and RMSECV of 2,15 %
 318 and RPD of 5,33 (model 8) which indicates that this model is suitable for estimating
 319 the moisture of the wood.

320 **Table 3:** Calibrations and cross-validations for the estimation of moisture in each class
 321 by PLS-R.

Model	Moisture	Treat	R ² c	RMSEc (%)	R ² CV	RMSECV (%)	RPD
7	0 - 40	-	0,96	2,22	0,95	2,34	4,80
8		1d	0,96	2,00	0,96	2,15	5,33
9	40 - 80	-	0,65	6,93	0,50	8,39	1,40
10		1d	0,71	6,27	0,46	8,99	1,31
11	> 80	-	0,81	7,54	0,69	9,55	1,82
12		1d	0,87	6,16	0,76	8,43	2,07

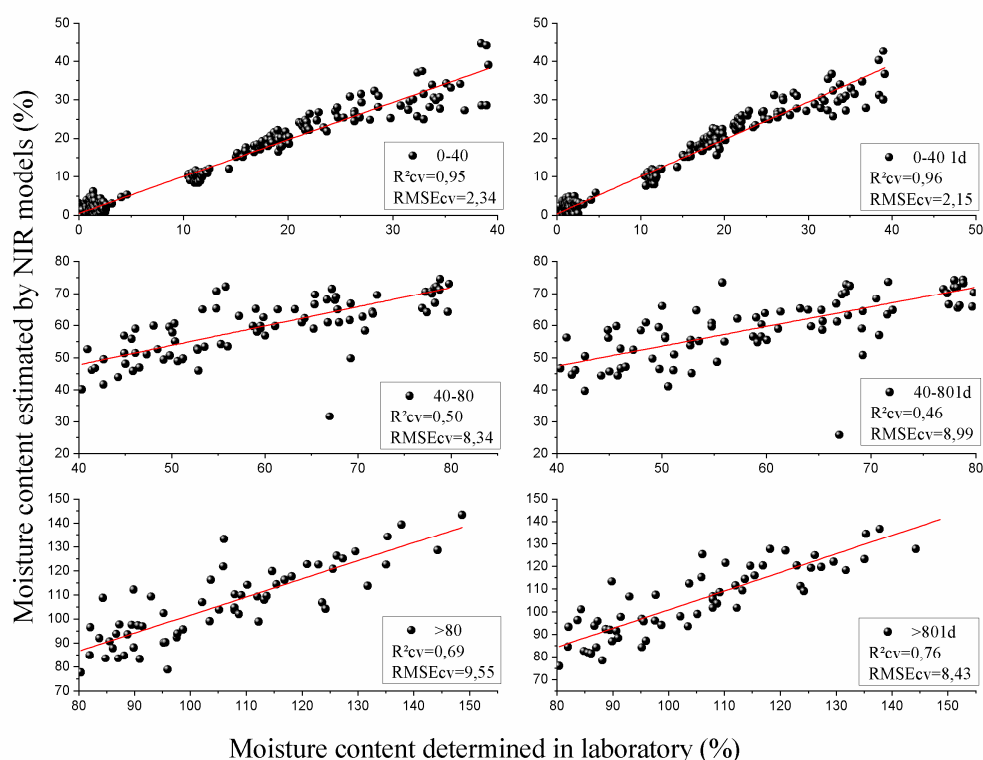
Treat - mathematical treatment; 1d - first derivative; R²c - coefficient of determination of the calibration; RMSEc - Root mean square error of calibration; R²CV - coefficient of determination of the cross validation; RMSECV - Root mean square error of cross-validation and RPD - ratio performance to deviation.

322

323 The moisture range of 40 % to 80 % was the one that showed the lowest performance
 324 with R²CV of 0,46 and RMSCV of 8,99 % and RPD of 1,40 (model 9), being considered
 325 unsatisfactory. RPD values greater than 1,5 are considered satisfactory in studies on
 326 forest sciences (Schimleck *et al.* 2003).

327 The third moisture class (> 80 %) provided a model with R²CV of 0,76 and
 328 RMSECV of 8,43 and RPD of 2,07, presenting better estimates than the second class
 329 of moisture, however, the error found is considered high, even though the RPD is
 330 indicating that the model is satisfactory. The best estimate found in this class was the
 331 treatment of the first derivative as well as in the first class of moisture. However, the
 332 second class of moisture that presented the lowest performance did not improve the
 333 model when performing the first derivative treatment in the spectra.

334 Figure 4 shows the plots made from the PLS-R in the three moisture ranges of
 335 original spectra and mathematically treated by the first derivative, collected from the
 336 longitudinal face through the integrator sphere acquisition path.



337 **Figure 4:** Moisture of the wood chips determined in laboratory and estimated from NIR
338 by integrating sphere of according to Table 3.

339
340 Figure 4 shows that the calibration values obtained from the spectra measured
341 in the 0 % to 40 % moisture range were more similar to those measured in the laboratory.
342 In this moisture range the spectra treated with the first derivative were the ones that
343 indicated the best model.

344 The moisture of 40 % to 80 % presented a lower adjustment of the data when
345 compared to the first and third moisture range. The third range of moisture also showed
346 a certain dispersion of the specimens when related to the actual values, however it
347 showed improvement when the first derivative treatment was performed.

348

349

350

351 **Test set validation of models for moisture estimation by class**

352 According to Pasquini (2003), external validation is recommended because it
 353 presents results that are closer to the real ones. Therefore, the models of the three
 354 moisture ranges were validated according to this method (Table 4).

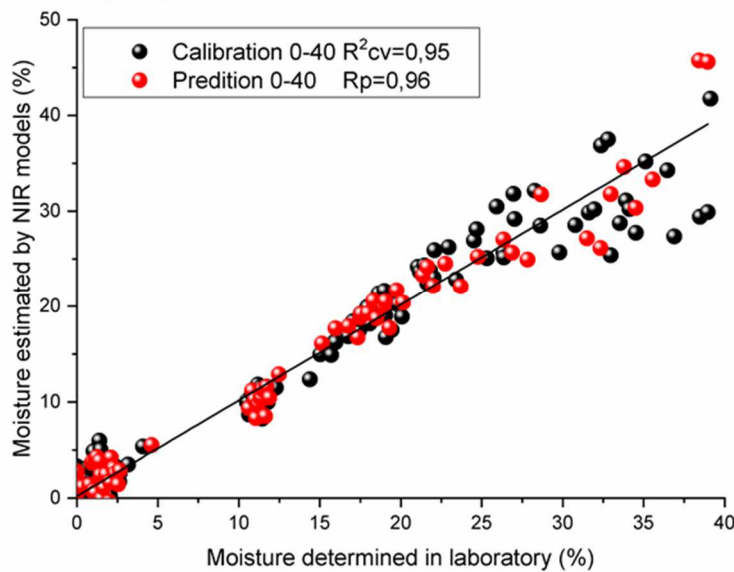
355 **Table 4:** Cross- and test set validations for the estimation of moisture in each class.

Moisture range (%)	R ² CV	RMSECV (%)	R ² p	RMSEP (%)	RPD
0-40	0,97	2,51	0,96	2,16	3,90
40-80	0,64	7,10	0,42	10,49	1,27
> 80	0,79	9,93	0,56	12,50	2,04

R²CV - coefficient of determination of the cross-validation; RMSECV - Root mean square error of cross validation; R²p - coefficient of determination of external validation; RMSEP – Root mean square error of external validation; RPD - standard deviation performance ratio.

356 From Table 3 and Table 4 it is possible to notice that the external validation
 357 values were similar to the values obtained through cross validation. However, most of
 358 the external validation values were inferior to those obtained in the cross validation.

359 Figure 5 shows the values obtained in the laboratory and predicted by the NIR,
 360 showing the distribution of the calibration points and the validation of the best model
 361 for estimating moisture in wood chips.



362 **Figure 5:** Regression of wood chips moisture values obtained in the laboratory and
 363 estimated in the NIR.

364 In order to improve the models, the initial specimens were separated according
 365 to the moisture of the wood and the wave numbers of 9000 cm⁻¹ to 12000 cm⁻¹ were
 366 excluded due to the occurrence of noise. However, as can be seen in Figure 5, only the
 367 first moisture range of 0 % to 40 % showed a strong correlation between the measured
 368 values and the predicted values, especially in moisture up to 25 %. This value is
 369 desirable for the pulp and paper industries, since the moisture in the wood chips should
 370 be above 25 %, but below 55 % for better use of the raw material in pulping and lower
 371 consumption of reagents.

372 **Partial Least Squares - Discriminant Analysis**

373 Table 5 lists the PLS-DA classifications, including the number of correct and
 374 incorrect classifications and the correct classification percentage by means of cross-
 375 validations. The confusion matrix (Table 5) shows that 343 from 400 (85,75 %) of
 376 specimens were correctly classified based on PLS-DA model.

377 **Table 5:** Confusion matrix of predictions of chip moisture through PLS-DA
 378 analysis.

Nominal Moisture classes (%)	Moisture estimated by NIR (%)			Correct classification		Total specimens
	0 - 40	40 - 80	> 80	No.	%	No.
0 - 40	253	3	0	253	98,83	256
40 - 80	26	43	14	43	51,81	83
> 80	0	14	47	47	77,05	61
Total	279	60	61	343	85,75	400

379
 380 Table 5 shows that in the first moisture class (0 to 40) %, composed of 256
 381 specimens, three of these specimens were incorrectly classified as belonging to the
 382 second moisture class, corresponding to 1,18 % of incorrect specimens. In the second
 383 class of moisture (40 to 80) %, 40 from 83 specimens were classified as incorrect; 26
 384 specimens were classified in the first moisture class and 14 specimens as the third

385 moisture class, corresponding to 48,20 % of specimens misclassified. In the third
386 moisture range (> 80 %), of the only 14 specimens were misclassified, which represents
387 22,96 % of incorrect specimens.

388 The class that classified the most specimens incorrectly was 40 % to 80 % of
389 moisture, while the class that obtained the most correct classifications was 0 % to 40 %
390 of moisture, presenting 98,82 % of correct classifications. Also, it is verified that none
391 of the specimens of the first class of moisture was classified as being of the third, and
392 the opposite also occurred. This can be explained by the large difference between these
393 two classes of moisture. Therefore, the specimens that were classified as incorrect could
394 present similar moisture in the classes that were assigned.

395 This study was carried out with the objective of verifying the feasibility of this
396 technique for rapid, immediate estimate of the moisture content in wood chips. The
397 promising findings of this approach open up new possibilities for applying NIR
398 spectroscopy in real situations, in which it is necessary to know the raw material
399 properties in real time for to optimizing the production process. One of the potential
400 applications would be on conveyors that take the chip from the pile to the digester in
401 pulp and paper mills. In this situation, the challenges are even greater, as chips with
402 different moisture, wood density and lignin content are mixed in the digester and the
403 resultant pulp must be as uniform as possible. Thus, more comprehensive studies
404 including chips with varying wood density and lignin content should be carried out to
405 reduce the distance from what is done under laboratory conditions and to real situations
406 in the pulp companies.

407

408 **CONCLUSIONS**

409 This study indicates that NIR spectroscopy associated with multivariate analysis
410 has the potential to estimate wood moisture in *Eucalyptus* chips. The model can be
411 generated from NIR spectral signatures obtained by integrator sphere and optical fiber.
412 The longitudinal face of the chips was shown to be more suitable for recording NIR
413 spectra and estimating the moisture in wood chips when compared to the transverse
414 face.

415 PLS-DA was able to correctly classified 85,75 % of the specimens in three
416 moisture classes. In each class, 98,82 % of specimens were correctly classified into the
417 group of drier specimens (0 to 40) % and 77,04 % of specimens were correctly grouped
418 in the class of wetter specimens (moisture > 80 %). PLS-DA models misclassified
419 48,20 % of specimens with moisture varying from 40 % to 80 %.

420 For PLS-R models, the estimates used for classifications of moisture classes
421 yielded better results. The percentage of correct classifications was 91 % when chips
422 were grouped into the three moisture classes based on the estimates originated from
423 PLS-R model.

424 This approach can be useful for the pulp and paper industries as it provides
425 accurate estimates of the moisture content of chips, assisting in the definition of cooking
426 parameters and optimizing industrial processes and the consumption of raw material
427 and reagents.

428 **ACKNOWLEDGEMENTS**

429 The authors thank the Wood Science and Technology Graduation Program
430 (DCF/UFLA, Brazil) for all the support for this study. The authors also thank Carlos
431 Henrique da Silva and Heber Dutra for technical support. This study was financed in

432 part by the Coordenação de Aperfeiçoamento de Pessoal de Nível Superior - Brasil
433 (CAPES) - Finance Code 001, by the Conselho Nacional de Desenvolvimento
434 Científico e Tecnológico (CNPq: grants n. 405085/2016-8) and by Fundação de
435 Amparo à Pesquisa do Estado de Minas Gerais (FAPEMIG). P.R.G. Hein was
436 supported by CNPq grants (process no. 303675/2017-9).

437

438 REFERENCES

439 **Adedipe, O.E.; Dawson-Andoh, B. 2008.** Predicting moisture content of yellow-
440 poplar (*Liriodendron tulipifera L.*) veneer using near infrared spectroscopy. *Forest*
441 *Prod J* 58(4): 28–33.

442 **Associação Brasileira de Normas Técnicas. ABNT. 2017.** NBR 14929: *Madeira:*
443 *determinação do teor de umidade de cavacos - Método por secagem em estufa.* ABNT,
444 Rio de Janeiro, Brasil. 3 p. <https://www.abntcatalogo.com.br/norma.aspx?ID=369854>

445 **Arriel, T.G.; Ramalho, F.M.G.; Lima, R.A.B.; Souza, K.I.R.; Hein, P.R.G.**
446 **Trugilho, P.F. 2019.** Developing near infrared spectroscopic models for predicting
447 density of Eucalyptus wood based on indirect measurement. *Cerne* 25(3): 294-300.
448 <https://doi.org/10.1590/01047760201925032646>

449 **Biermann, C. J. 1996.** *Handbook of Pulping and Papermaking.* 2nd Ed. Academic
450 Press. San Diego, USA. 754p. <https://doi.org/10.1016/B978-0-12-097362-0.X5000-6>

451 **Costa, E.V.S.; Rocha, M.F.V.; Hein, R.G.; Amaral, E.A.; Santos, L.M.; Brandão,**
452 **L.E.V.S.; Trugilho, P.F. 2018.** Influence of spectral acquisition technique and wood
453 anisotropy on the statistics of predictive near infrared–based models for wood density.
454 *J Near Infrared Spec* 26(2): 106-116. <https://doi.org/10.1177/0967033518757070>

455 **Dahlbacka, J. Lillhonga, T. 2010.** Moisture measurement in timber utilising a multi-
456 layer partial least squares calibration approach. *J Near Infrared Spec* 18(6): 425-432.
457 <https://doi.org/10.1255/jnirs.906>

458 **Defo, M.; Taylor, A.M.; Bond, B. 2007.** Determination of moisture content and
459 density of fresh-sawn red oak lumber by near infrared spectroscopy. *Forest Prod J*
460 57(5): 68-72.

461 **Eom, C.D.; Park, J.H.; Choi, I.G.; Choi, J.W.; Han, Y.; Yeo, H. 2013.**
462 Determining surface emission coefficient of wood using theoretical methods and
463 near-infrared spectroscopy. *Wood Fiber Sci* 45(1): 76–83.
464 <https://wfs.swst.org/index.php/wfs/article/view/522>

- 465 **Fardim, P.; Ferrreira, M.M.C.; Duran, N. 2005.** Determination of mechanical and
466 optical properties of *Eucalyptus* kraft pulp by NIR spectrometry and multivariate
467 calibration. *J Wood Chem Technol* 25(4): 267–279.
468 <https://doi.org/10.1080/02773810500366748>
- 469 **Fujimoto, T.; Kobori, H.; Tsuchikawa, S. 2012.** Prediction of wood density
470 independently of moisture conditions using near infrared spectroscopy. *J Near*
471 *Infrared Spec* 20(3): 353-359. <https://doi.org/10.1255/jnirs.994>
- 472 **Gomide, J.L.; Fantuzzi Neto, H. 2000.** Aspectos fundamentais da polpação Kraft de
473 madeira de *Eucalyptus*. *O Papel* 3(61): 62-68.
- 474 **Karttunen, K.; Leinonen, A.; Saren, M. 2008.** A survey of moisture distribution in
475 two sets of Scots pine logs by NIR-spectroscopy. *Holzforschung* 62(4): 435-440.
476 <https://doi.org/10.1515/HF.2008.060>
- 477 **Martens, H.; Naes, T. 1991.** *Multivariate calibration*. 1st Ed. John Wiley & Sons. New
478 York, USA. 419p.
- 479 **Muñiz, G.I.; Magalhães, W.L.E.; Carneiro, M.E.; Viana, L.C. 2012.** Fundamentos
480 e estado da arte da Espectroscopia no Infravermelho Próximo no setor de base florestal.
481 *Cienc Florest* 22(4): 865-875. <http://dx.doi.org/10.5902/198050987567>
- 482 **Nunes, C.A.; Freitas, M.P; Pinheiro, A.C.M.; Bastos, S.C. 2012.** Chemoface: a
483 novel free user-friendly interface for chemometrics. *J Brazil Chem Soc* 23(11): 2003-
484 2010. <https://doi.org/10.1590/S0103-50532012005000073>
- 485 **Pasquini, C. 2003.** Near infrared spectroscopy: fundamentals, practical aspects and
486 analytical applications. *J Brazil Chem Soc* 14(2): 198-219.
487 <https://doi.org/10.1590/S0103-50532003000200006>
- 488 **Pasquini, C. 2018.** Near Infrared Spectroscopy: a mature analytical technique with new
489 perspectives – A review. *Anal Chim Acta* 1026: 8-36.
490 <https://doi.org/10.1016/j.aca.2018.04.004>
- 491 **Pavia, D.L.; Lampman, G.M.; Kriz, G.S.; Vyvyan, J.R. 2010.** *Introdução a*
492 *espectroscopia*. 4th Ed. Cengage Learning. São Paulo, Brazil. 716p.
493 [https://www.cengage.com.br/learning-solutions/introducao-a-espectroscopia-](https://www.cengage.com.br/learning-solutions/introducao-a-espectroscopia-traducao-da-4a-edicao-norte-americana/)
494 [traducao-da-4a-edicao-norte-americana/](https://www.cengage.com.br/learning-solutions/introducao-a-espectroscopia-traducao-da-4a-edicao-norte-americana/)
- 495 **Price, N.C.; Dwek, R.A.; Wormald, M.; Ratcliffe, R.G. 2001.** *Principles and*
496 *problems in physical chemistry for biochemists*. 3rd Ed. Oxford University Press.
497 Oxford, UK. 401p.
- 498 **Rosado, L.R.; Takarada, L.M.; Araújo, A.C.C.; Souza, K.R.D.; Hein, P.R.G.;**
499 **Rosado, S.C.S.; Gonçalves, F.M.A. 2019.** Near infrared spectroscopy: rapid and

- 500 accurate analytical tool for prediction of non-structural carbohydrates in wood. *Cerne*
501 25(1): 84-92. <https://doi.org/10.1590/01047760201925012614>
- 502 **Santos, L.M. 2017.** *Monitoramento da dessecção de água na madeira por*
503 *espectroscopia no infravermelho próximo.* Master thesis. Universidade Federal de
504 Lavras, Lavras. 56 p.
- 505 **Schimleck, L.R.; Doran, J.C.; Rimbawanto, A. 2003.** Near infrared spectroscopy for
506 cost effective screening of foliar oil characteristics in a *Melaleuca cajuputi* breeding
507 population. *J Agric Food Chem* 51(9): 2433-2437. <https://doi.org/10.1021/jf020981u>
- 508 **Sobering, D.C.; Williams, C. 1993.** Comparison of commercial near infrared
509 transmittance and reflectance instruments for analysis of whole grains and seeds. *J Near*
510 *Infrared Spec* 1(1): 25-33.
511 <https://www.osapublishing.org/jnirs/abstract.cfm?URI=jnirs-1-1-25>
- 512 **Tham, V.T.H.; Inagaki, T.E.; Tsuchikawa, S. 2018.** A novel combined application
513 of capacitive method and near-infrared spectroscopy for predicting the density and
514 moisture content of solid wood. *Wood Sci Technol* 52(1): 115-
515 129. <https://doi.org/10.1007/s00226-017-0974-x>
- 516 **Thygesen, L.G.; Lundqvist, S.O. 2000.** NIR Measurement of Moisture Content in
517 Wood under Unstable Temperature Conditions. Part 1. Thermal Effects in near Infrared
518 Spectra of Wood. *J Near Infrared Spec* 8(3):183-189. <https://doi.org/10.1255/jnirs.277>
- 519 **Tsuchikawa, S.; Kobori, H. 2015.** A review of recent application of near infrared
520 spectroscopy to wood science and technology. *J Wood Sci* 61(3): 213–220.
521 <https://doi.org/10.1007/s10086-015-1467-x>
- 522 **Tsuchikawa, S.; Schwanninger, M. 2013.** A review of recent near-infrared research
523 for wood and paper (Part 2). *Appl Spectrosc Rev* 48(7): 560-587.
524 <https://doi.org/10.1080/05704928.2011.621079>
- 525 **Tyson, J.A.; Schimleck, L.R.; Aguiar, A.M.; Abad, J.I.M.; Rezende, G.D.S.P;**
526 **Filho, O.M. 2012.** Development of near infrared calibrations for physical and
527 mechanical properties of eucalypt pulps of mill-line origin. *J Near Infrared Spec* 20(2):
528 287-294. <https://doi.org/10.1255/jnirs.988>
- 529 **Watanabe, K.; Mansfield, S. D.; Avramidis, S. 2011.** Application of near-infrared
530 spectroscopy for moisture-based sorting of green, hem-fir timber. *J Wood Sci* 57(4):
531 288-294. <https://doi.org/10.1007/s10086-011-1181-2>
- 532 **Yang, L.; Liu, H.; Cai, Y.; Hayashi, K.; Wu, Z. 2014.** Effect of drying conditions on
533 the collapse-prone wood of *Eucalyptus urophylla*. *BioResources* 9(4): 7288-7298.
534 <https://doi.org/10.15376/biores.9.4.7288-7298>

535 **Zhang, M.; Liu, Y.; Yang, Z. 2015.** Correlation of near infrared spectroscopy
536 measurements with the surface roughness of wood. *BioResouces* 10(4): 6953-6960.
537 <https://doi.org/10.15376/biores.10.4.6953-6960>

Accepted manuscript